JMEPEG (2012) 21:1455–1461
DOI: 10.1007/s11665-011-0031-0

1059-9495/$19.00

Research on Flow Stress During Hot Deformation Process and Processing Map for 316LN Austenitic Stainless Steel

Baofeng Guo, Haipeng Ji, Xingang Liu, Lu Gao, Rongmei Dong, Miao Jin, and Qinghua Zhang

(Submitted December 28, 2010; in revised form July 23, 2011)

In this study, the hot deformation behavior of austenitic stainless steel was investigated using Gleeble-3500 thermomechanical simulator at deformation temperatures in the range of 900-1200 °C and strain rates in the range of 0.001-10 s^{-1}. The effects of initial austenitic grain size and deformation conditions on hot deformation behavior of 316LN were analyzed through true stress-strain curves under different deformation conditions. Both the constitutive equation and processing map for 316LN were obtained. The results show that, with the increase of the deformation temperature and the decrease of the strain rate, the peak stress decreases, and the initial austenitic grain size has a little influence on the peak stress. The relative error between the peak stress values calculated using the constitutive equation and the values measured is less than 10%. Using the processing map, the best hot-working condition for 316LN in the range of experimental deformation parameters appears when $T = 1200$ °C and $\dot{\varepsilon} = 0.001\ s^{-1}$.

Keywords forging, modeling processes, stainless steels

1. Introduction

316LN austenitic stainless steel featuring excellent corrosion resistance, high temperature mechanical properties, work hardening ability, and impact toughness is used as the material of main pipes in AP1000 (AP means Advanced Passive, 1000 means 1000 megawatts of electricity) which is based on the technology of third generation pressurized water reactor developed by the Westinghouse Electric Corporation in America.

The hot deformation behaviors of 316- and 316L- in 316-type stainless steels have been well studied (Ref 1–7), but little has been reported on 316LN. 316LN, which has a larger strength, can be obtained by adding the element N on the basis of the characteristics of 316L. Although other characteristics of 316LN, such as fatigue damage resistance, corrosion resistance, and microstructure, have been widely researched (Ref 8–14), the hot deformation behavior has not received sufficient attention. Nevertheless, the primary coolant pipes in AP1000 nuclear power station reactor and other nuclear forgings using 316LN as material require higher grain size, and the samples produced so far have not reached the required standard; 316LN is an austenitic stainless steel the grain refinement of which can be achieved only through the hot deformation process. Therefore, the hot deformation behavior of 316LN needs to be studied in-depth more to provide theoretical basis for process determination.

Baofeng Guo, Haipeng Ji, Xingang Liu, Lu Gao, Rongmei Dong, and **Miao Jin**, Yanshan University, Qinhuangdao 066004, China; and **Qinghua Zhang**, China National Erzhong Group Co., Deyang 618013, China. Contact e-mail: lxg@ysu.edu.cn.

2. Material and Experimental Procedure

2.1 Testing Material

The chemical composition of the steels used in the experiment is given in Table 1. The specimens were from the trial product (which is manufactured by a nuclear forging manufacture) of the primary coolant pipes in AP1000 nuclear power station reactor.

2.2 Experimental Procedure

The samples used in the tests were cylindrical specimens of 8 mm in diameter and 12 mm in length. The hot compression tests were carried out on Gleeble-3500 thermomechanical simulator. In order to decrease the friction effects in the deformation process, high-temperature lubricant was applied, and tantalum plates were placed onto both ends of the specimens.

The specimens were heated to 1250 °C at a rate of 10 °C/s, held for 5 min to obtain the same initial austenitic grain size, cooled to deformation temperatures at a rate of 10 °C/s, thermally retarded for 30 s, and then subjected to compressive deformation at different strain rates. The deformations were performed at temperatures ranging from 900 to 1200 °C at 50 °C intervals. The strain rates used were 0.001, 0.01, 0.1, 1, and 10 s^{-1}, and the deformation value was 70%.

In order to investigate the effects of initial austenitic grain size on flow stress of 316LN, a total of 27 different tests were performed under various conditions covering the total possible combinations of three different heated temperatures, three different deformation temperatures, and three different strain rates at which the deformation processes were carried out. The specimens were, heated to 1150, 1200 and 1250 °C, held for 5 min to obtain different initial austenitic grain sizes, cooled to the specified deformation temperatures at a rate of 10 °C/s, and then subjected to compressive deformation at specified strain rates. The three deformation temperatures were 950, 1050 and

Table 1 Main chemical composition of 316LN for test (%)

Elements	C	Si	Mn	S	P	Cr	Ni	Mo	N
Content	≤0.03	≤1.00	≤2.00	≤0.03	≤0.035	≤16.00-18.50	≤10.50-14.50	≤2.00-3.00	≤0.12-0.22

1150 °C. The three strain rates used were 0.01, 0.1 and 1 s^{-1}, and the deformation value was 50%.

3. Results and Discussion

Figure 1 shows the true stress-strain curves of 316LN obtained from the experiments at different deformation temperatures and strain rates. These true stress-strain curves can be divided into dynamic recovery type and dynamic recovery plus dynamic recrystallization type.

The true stress-strain curve of 316LN is dynamic recovery plus dynamic recrystallization type at deformation temperature of 900 °C and strain rate of 0.01 s^{-1}, see Fig. 1(a). It can be seen from the curve that, when the true strain ε is smaller than 0.01, the true stress increases rapidly with the increase of true strain because of the dominant effect of work hardening. When the true strain ε is larger than 0.01, the growth of true stress values slows down owing to dynamic recovery. With deformation going on, the softening effect is more significant than hardening due to dynamic recrystallization. The true stress decreases after reaching the peak value, and then keeps a steady state as softening and hardening effects are basically in balance.

The true stress-strain curve of 316LN is dynamic recovery type at deformation temperature of 1100 °C and strain rates of 10 s^{-1}, see Fig. 1(b). It can be seen from the curve that, when the true strain ε is smaller than 0.03, the true stress increases rapidly with the increase of true strain because of the dominant effect of work hardening. When the true strain ε is larger than 0.03, although the true stress continues to increase with the increase of true strain, softening makes the growth of true stress values slow down owing to the dynamic recovery. Nevertheless, there is no obvious peak stress in these curves, as dynamic recrystallization never or rarely occurs in the deformation process.

3.1 Effect of Deformation Parameters on the Flow Stress

It can be seen from Fig. 1(a) that dynamic recrystallization occurs at all deformation temperatures at the strain rate of 0.01 s^{-1}, and the stress values decrease with the increase of deformation temperature when the strain values are the same. Figure 2 shows the effect of deformation temperature on peak stress at a specific strain rate ($\dot{\varepsilon} = 0.01\ s^{-1}$). As shown in the figure, when the deformation temperature is 900 °C, the peak stress is 208 MPa, and when the deformation temperature increases to 1200 °C, the peak stress decreases to 53 MPa. In other words, the peak value decreases with the increase of the deformation temperature. Furthermore, the decreasing rate of flow stress gradually deceases with the increase of deformation temperature, i.e., the higher the deformation temperature, the lower the sensitivity of flow stress on temperature.

Figure 3 shows the effect of strain rate on peak stress. It can be seen from this figure that, at the same deformation temperature of 1100 °C, the peak stress is 48 MPa at strain rate of 0.001 s^{-1}; it increases to 210 MPa when the strain rate rises to 10 s^{-1}. It can be concluded that, at the same deformation temperature, the lower the strain rate, the smaller the peak stress.

3.2 Effect of Initial Austenitic Grain Size on the Flow Stress

Figure 4 shows the grain microstructures, which were obtained through water quenching after the materials were, respectively, heated to 1150, 1200 and 1250 °C and held for 5 min. The resulting initial austenitic grain sizes of the specimens measured using transversal method are 50, 120, and 185 μm, respectively.

Figure 5 shows the effect of initial austenitic grain size on peak stress. It is seen that, under the deformation conditions of $T = 1050$ °C and $\dot{\varepsilon} = 0.01\ s^{-1}$, the peak stresses corresponding to the initial austenitic grain sizes of 50 and 120 μm differ by 12%, and the peak stresses corresponding to 120 and 185 μm differ by 8%. Under another deformation condition of $T = 1150$ °C and $\dot{\varepsilon} = 0.1\ s^{-1}$, similarly, the peak stresses corresponding to 50 and 120 μm differ by 4%, and the values corresponding to 120 and 185 μm differ by 1%. These results indicate that the initial austenitic grain size only has a slight influence on the peak stress (Ref 15, 16).

4. Establishment of Constitutive Equation for 316LN

Sellars and McTegart (Ref 17) considered that the relationship among flow stress, deformation temperature, and strain rate in the plastic deformation process of metallic materials at high temperature can be expressed by hyperbolic sine form including deformation activation energy Q and deformation temperature T, shown as follows:

$$\dot{\varepsilon} = A_0 f(\sigma) \exp(-Q/RT) \quad \text{(Eq 1)}$$

where $f(\sigma)$ represents stress function, $\dot{\varepsilon}$ is strain rate, σ is stress (in this article, it represents peak stress), Q is deformation activation energy, T is thermodynamics temperature, R is gas constant (R = 8.314 J/(mol·K)), and A_0 is a constant. $f(\sigma)$ can be expressed by the following equation:

$$\text{a.}\quad f(\sigma) = \sigma^{n_1}, \quad \text{under lower stress } (\alpha\sigma < 0.8); \quad \text{(Eq 2)}$$

$$\text{b.}\quad f(\sigma) = \exp(\beta\sigma), \quad \text{under higher stress } (\alpha\sigma > 1.2); \quad \text{(Eq 3)}$$

$$\text{c.}\quad f(\sigma) = [\sinh(\alpha\sigma)]^n, \quad \text{under all stress.} \quad \text{(Eq 4)}$$

By substituting of Eq 2 and 3 into Eq 1, we have

$$\dot{\varepsilon} = A_1 \sigma^{n_1} \exp(-Q/RT) \quad \text{(Eq 5)}$$

$$\dot{\varepsilon} = A_2 \exp(\beta\sigma) \exp(-Q/RT) \quad \text{(Eq 6)}$$

By substituting of Eq 4 into Eq 1, we have

$$\dot{\varepsilon} = A[\sinh(\alpha\sigma)]^n \exp(-Q/RT) \quad \text{(Eq 7)}$$

where n represents strain hardening exponent, and n_1, β, α, A_1, A_2, and A are the constants determined by deformation.

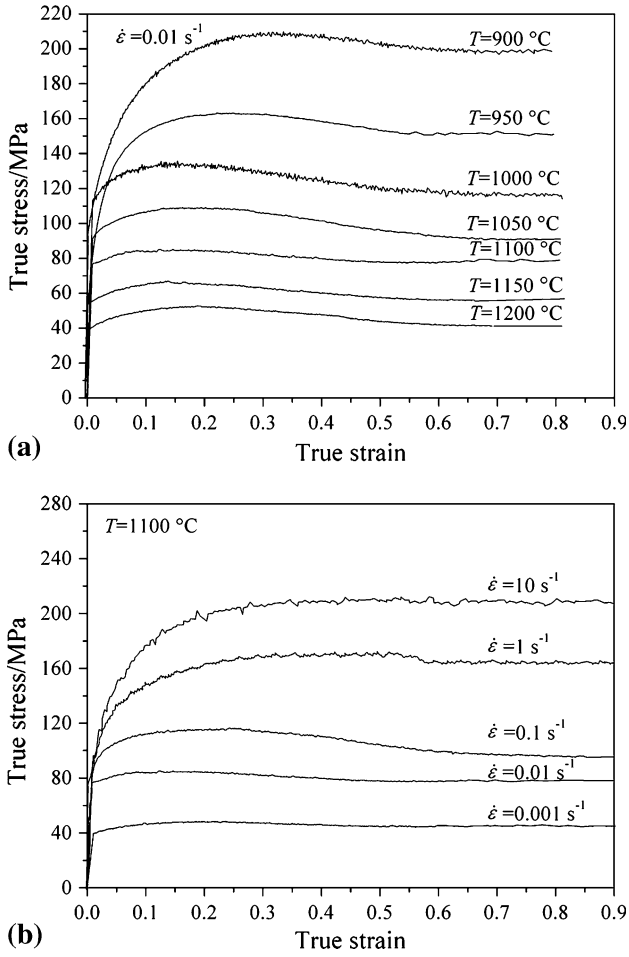

Fig. 1 True stress-strain curves at different deformation temperatures and strain rates. (a) For different deformation temperatures at $\dot{\varepsilon} = 0.01\ s^{-1}$. (b) For different strain rates at $T = 1100$ °C

$$\alpha = \frac{\beta}{n_1} \quad \text{(Eq 8)}$$

where T and $\dot{\varepsilon}$ are deformation parameters set by experiment, σ is obtained from the experiment; n_1, β, α, n, Q, and A are the parameters needed to be determined.

Zener and Hollomon (Ref 18) found that the relationship between stress and strain of steel material cannot be fully determined by the material characteristics only. It is also related to the deformation temperature T and strain rate $\dot{\varepsilon}$. The relationship between T and $\dot{\varepsilon}$ can be expressed using parameter Z as follows:

$$Z = \dot{\varepsilon}\exp(Q/RT) = A[\sinh(\alpha\sigma)]^n \quad \text{(Eq 9)}$$

The physical meaning of parameter Z is temperature compensation of the strain rate factor.

According to Eq 7 and 9, the constitutive equation can be expressed using parameter Z as follows:

$$\sigma = (1/\alpha)\ln\left\{(Z/A)^{1/n} + \left[(Z/A)^{2/n} + 1\right]^{1/2}\right\} \quad \text{(Eq 10)}$$

4.1 Solution of Parameters

Take the logarithm of both sides of Eq 5, and plot the curve between $\ln\dot{\varepsilon}$ and $\ln\sigma$. When the deformation temperature T is specified, the slope of the straight line, which represents n_1 at the corresponding temperature, can be obtained by linear regression. Through averaging the multiple n_1 obtained by changing T, the value of n_1 (n_1 = 6.56607) can be obtained. Similarly, the value of β (β = 0.0556) can be solved. According to n_1 and β, α can be solved: ($\alpha = \frac{\beta}{n_1} = 0.008468$).

Take the logarithm of both sides of Eq 7, and plot the curve between $\ln\dot{\varepsilon}$ and $\ln[\sinh(\alpha\sigma)]$ under different deformation temperatures (as shown in Fig. 6). The slopes of the straight lines corresponding to different deformation temperatures can be obtained by linear regression. Through averaging the slopes, strain hardening exponent n can be solved (n = 4.69141).

Take the logarithm of both sides of Eq 7, and plot the curve between $\ln[\sinh(\alpha\sigma)]$ and $1/T$ at a constant strain rate $\dot{\varepsilon}$ (as shown in Fig. 7). The slope of the straight line at the corresponding strain rate, which equals the rate between Q and Rn, can be obtained by linear regression. The value of Q/Rn (Q/Rn = 11764) can be solved through averaging the multiple Q/Rn obtained by changing the strain rates. By substituting R = 8.314 J/(mol·K) and n = 4.69141 into Q/Rn, Q can be determined as 458848 J/mol.

The deformation activation energy Q and strain hardening exponent n of 316, 316L, and 316LN in 316-type austenitic stainless steel from the references are shown in Table 2. It shows that the values of Q mainly vary over the range from 410,000 to 490,000 J/mol. The deformation activation energy

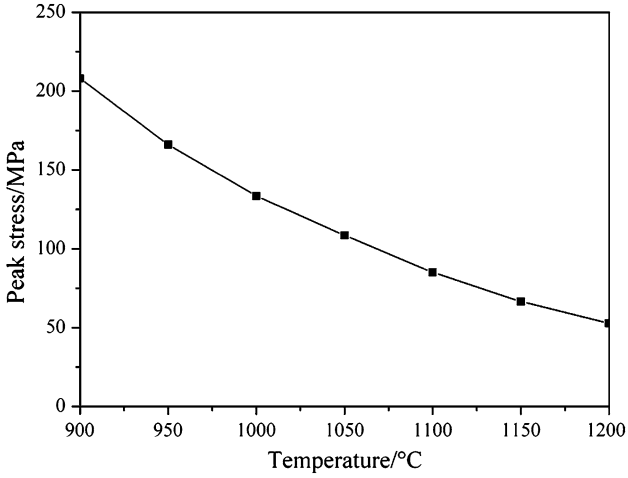

Fig. 2 Effect of deformation temperature on peak stress at $\dot{\varepsilon} = 0.01\ s^{-1}$

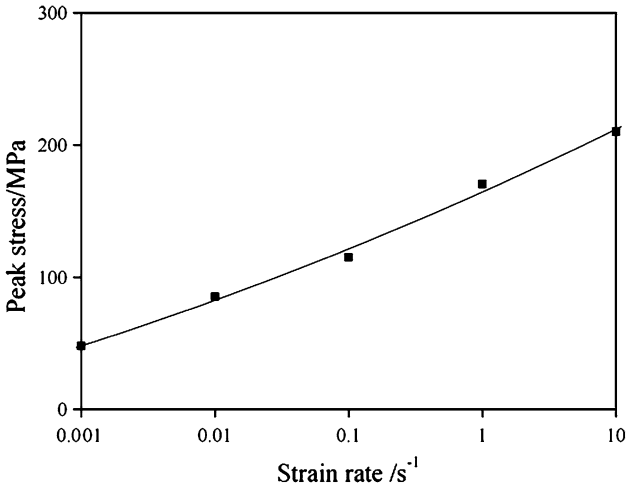

Fig. 3 Effect of strain rate on peak stress at $T = 1100$ °C

of 316LN given in this study is close to those of both 316 (Ref 5) and 316L (Ref 6). It can be seen that there are no obvious changes in the deformation activation energy among 316, 316L, and 316LN, and the value of n varies between 4.00 and 5.00.

4.2 Establishment of Constitutive Equation

By substituting strain rate $\dot{\varepsilon}$, deformation temperature T, gas constant R, and deformation activation energy Q into Eq 9, the corresponding parameter Z can be obtained.

Take the logarithm of both sides of Eq 9, and the following equation can be obtained.

$$\ln Z = n \ln[\sinh(\alpha\sigma)] + \ln A \quad \text{(Eq 11)}$$

Plot the curve between $\ln Z$ and $\ln[\sinh(\alpha\sigma)]$ (as shown in Fig. 8), and straight intercept ($\ln A = 37.276$) can be obtained by linear regression. Then, A, whose value is 1.54×10^{16}, can be obtained.

As discussed above, the relationship among flow stress, deformation temperature, and strain rate in the hot deformation process of 316LN can be expressed as follows:

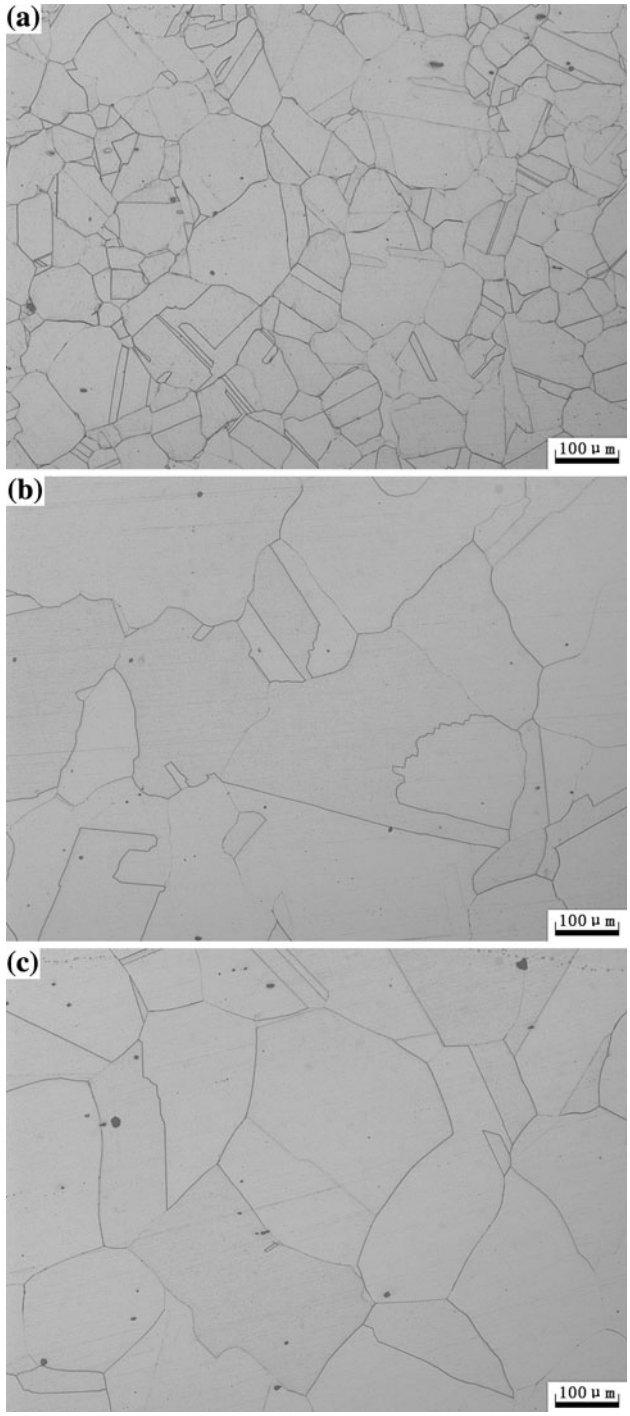

Fig. 4 Microstructures of 316LN at different heating temperatures. (a) 1150 °C. (b) 1200 °C. (c) 1250 °C

$$\dot{\varepsilon} = 1.54 \times 10^{16}[\sinh(0.008468\sigma)]^{4.7} \exp(-55190/T) \quad \text{(Eq 12)}$$

The expression of parameter Z is as follows:

$$Z = \dot{\varepsilon} \exp(55190/T) = 1.54 \times 10^{16}[\sinh(0.008468\sigma)]^{4.7} \quad \text{(Eq 13)}$$

By substituting the calculated parameters into Eq 10, constitutive equation for 316LN can be expressed as follows:

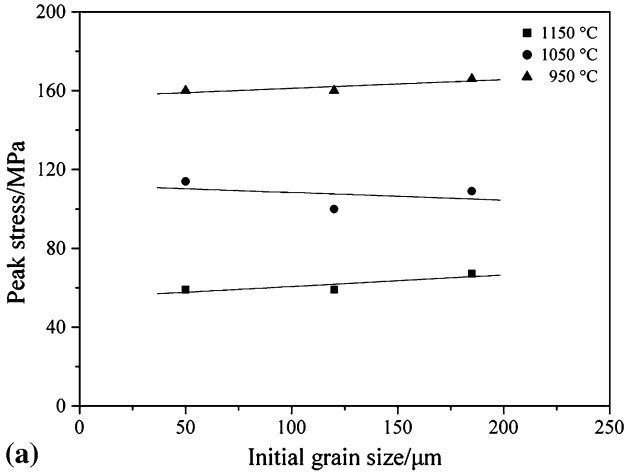

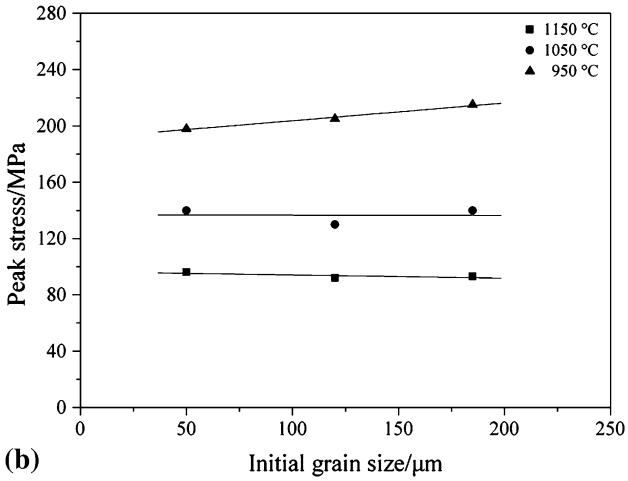

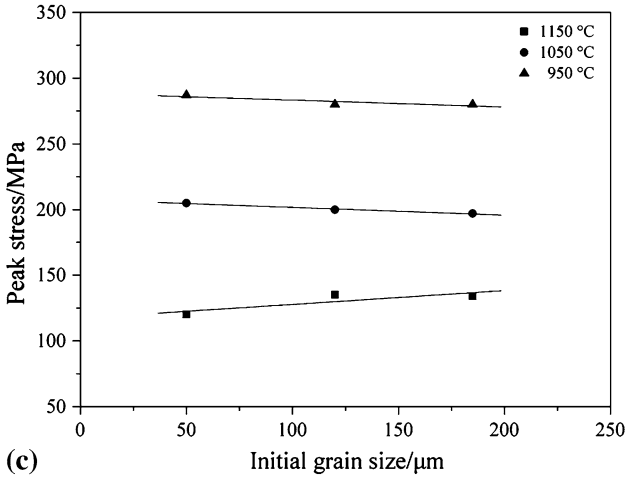

Fig. 5 Effect of initial austenitic grain size on peak stress. (a) $\dot{\varepsilon} = 0.01\ s^{-1}$. (b) $\dot{\varepsilon} = 0.1\ s^{-1}$. (c) $\dot{\varepsilon} = 1\ s^{-1}$

$$\sigma = (1/0.008468)\ln\left\{(Z/A)^{1/4.7} + \left[(Z/A)^{2/4.7} + 1\right]^{1/2}\right\} \quad \text{(Eq 14)}$$

By substituting the deformation parameters from the experiment into Eq 14, the difference in the values between the calculated peak stress and the data measured by experiment,

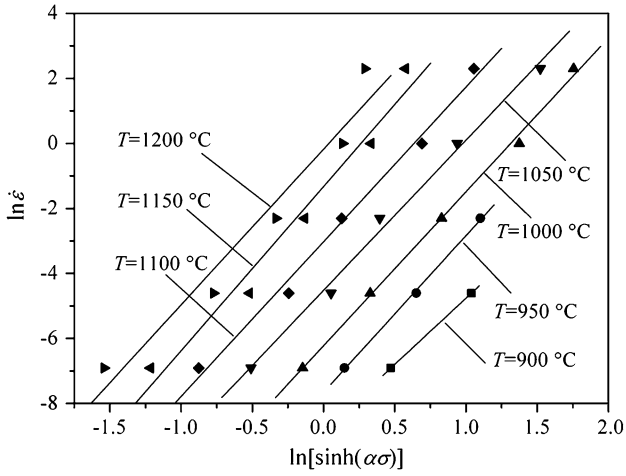

Fig. 6 Relationship between strain rate and stress at different deformation temperatures

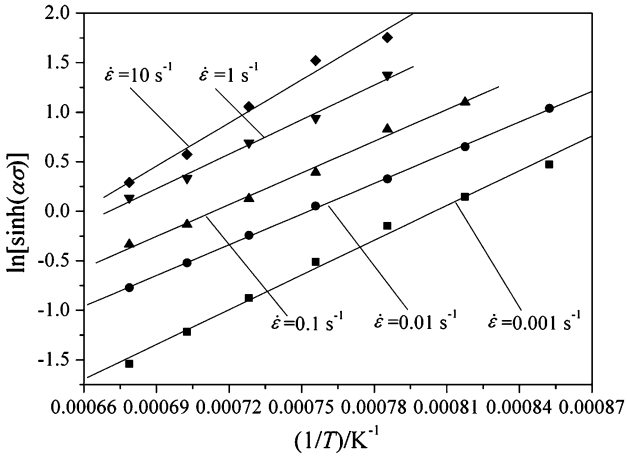

Fig. 7 Relationship between deformation temperature and stress at different strain rates

which is within 10%, are shown in Fig. 9. Therefore, it can be considered that the constitutive equation is comparatively accurate.

5. Processing Map of 316LN

Dissipative structure theory regards that the energy received by per unit volume of material in machining process equals the product of stress and strain rate. However, dynamic material model (Ref 20) presumes that the total power dissipated by workpiece at any time consists of G content and J co-content (Ref 21), where G content represents the power dissipated by plastic deformation, and J co-content represents the power dissipated by microstructure change. The mathematical description is

$$P = \sigma\dot{\varepsilon} = G + J = \int_0^{\dot{\varepsilon}} \sigma d\dot{\varepsilon} + \int_0^{\sigma} \dot{\varepsilon} d\sigma \quad \text{(Eq 15)}$$

Based on dynamic material model, constitutive equation can be expressed as

Table 2 Comparison of Q and n of 316, 316L and 316LN

Material	Deformation activation energy Q, J/mol	Strain hardening exponent, n	Reference
316	413,800	4.93	Ref 4
316	460,000	4.30	Ref 5
316L	450,218	4.12	Ref 6
316LN	485,000	5.70	Ref 19
316LN	458,848	4.70	This study

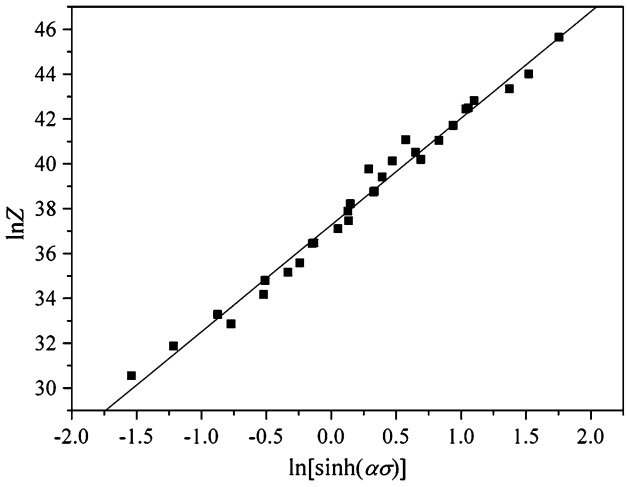

Fig. 8 Relationship between parameter Z and stress

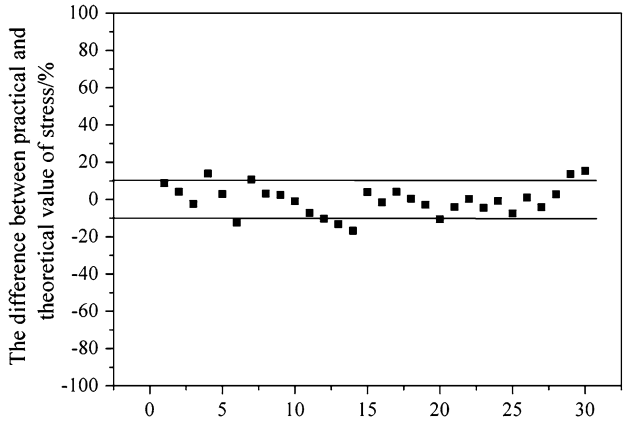

Fig. 9 The difference between measured and calculated values of stress

$$\sigma = K \cdot \dot{\varepsilon}^m \quad \text{(Eq 16)}$$

where σ is stress, $\dot{\varepsilon}$ is strain rate, K is a constant, and m is the sensitivity coefficient of strain rate.

From Eq 15 and 16, it can be concluded as follows:

$$m = \left[\frac{\partial(\ln\sigma)}{\partial(\ln\dot{\varepsilon})}\right]_{\varepsilon,T} = \left[\frac{\dot{\varepsilon}\partial\sigma}{\sigma\partial\dot{\varepsilon}}\right]_{\varepsilon,T} = \left[\frac{\partial J}{\partial G}\right]_{\varepsilon,T} \quad \text{(Eq 17)}$$

Therefore, the sensitivity coefficient of strain rate m determines the distribution relation between G and J

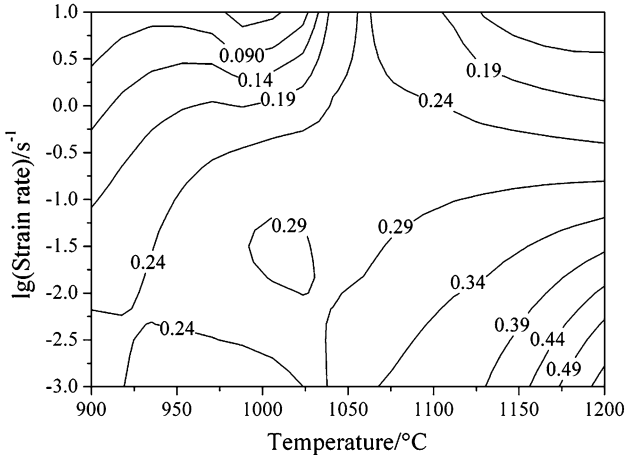

Fig. 10 Dissipation efficiency map for 316LN obtained at strain of 0.5

(Ref 21, 22). As for the ideal linear dissipation, when $m = 1$, the maximum value of J is as follows:

$$J_{\max} = P/2 \quad \text{(Eq 18)}$$

when the ratio of co-content and its maximum value is defined as the dissipation factor η:

$$\eta = \frac{J}{J_{\max}} \quad \text{(Eq 19)}$$

From Eq 15, 18 and 19, the following equation can be obtained:

$$\eta = \frac{P-G}{P/2} = 2\left(1 - \frac{1}{\sigma\dot{\varepsilon}}\int_0^{\dot{\varepsilon}} \sigma d\dot{\varepsilon}\right) \quad \text{(Eq 20)}$$

$$\text{while} \quad \int_0^{\dot{\varepsilon}} \sigma d\dot{\varepsilon} = \int_0^{\dot{\varepsilon}} K\dot{\varepsilon}^m d\dot{\varepsilon} = \frac{K\dot{\varepsilon}^m\dot{\varepsilon}}{1+m} = \frac{\sigma\dot{\varepsilon}}{1+m} \quad \text{(Eq 21)}$$

$$\eta = 2\left(1 - \frac{1}{1+m}\right) = \frac{2m}{1+m} \quad \text{(Eq 22)}$$

The efficiency of power dissipation that is a non-dimensional parameter represents the proportion of the power dissipated by microstructure evolution to total power. The power dissipated by microstructure evolution increases with the increase of the value of η, i.e., the deformation process needs more energy for dynamic recrystallization, and the maximum value of η appears in the region of dynamic recrystallization (Ref 21). The contour map that η varies with the variation of deformation temperature and strain rate is the power dissipation map, which is important part of hot processing map, and the map is an important reference for the determination of the best technological parameters of hot deformation in a hot-working process.

Figure 10 shows the power dissipation map of 316LN at true strain of 0.5. It shows that the values of efficiency of power dissipation η are generally larger in the region of higher temperature and lower strain rate, i.e., the power used for microstructure evolution in hot deformation process in this region is more than those in the other regions. When hot deformation of 316LN is carried out in the region of higher

temperature and lower strain rate, complete dynamic recrystallization occurs; therefore, this is the preferred hot-working region for the material. The efficiency of power dissipation η is small in the region of lower temperature and higher strain rate, as dynamic recovery or partial dynamic recrystallization occurs if hot deformation is carried out in the region.

For example, under the deformation condition of $T = 1100$ °C, $\dot{\varepsilon} = 0.001$ s^{-1} and $\eta = 0.37$ (as shown in Fig. 1(b)), complete dynamic recrystallization occurs; and when T is 1100 °C, $\dot{\varepsilon}$ is 10 s^{-1} and η is 0.20, only dynamic recovery occurs; and when T is 900 °C, $\dot{\varepsilon}$ is 0.01 s^{-1} and η is 0.27 (as shown in Fig. 1(a)), partial dynamic recrystallization occurs.

Figure 10 shows that the maximum value of η in the range of experimental deformation parameters appears at $T = 1200$ °C and $\dot{\varepsilon} = 0.001$ s^{-1}. Hence, this is the best hot-working condition for 316LN.

6. Conclusions

Based on the results and discussion on hot deformation experiments at temperatures of 900-1200 °C with strain rates of 0.001-10 s^{-1}, the basic conclusions can be drawn as follows:

1. In the range of experimental deformation parameters of 316LN, the higher the deformation temperature and the lower the strain rate, the smaller the peak stress of flow stress. The initial austenitic grain size has a slight influence on peak stress.
2. When deformation activation energy Q and strain hardening exponent n of 316LN during hot deformation are 458848 and 4.69141 J/mol, respectively, the constitutive equation for 316LN can be expressed as Eq 13 and 14.
3. According to the power dissipation map of 316LN, the region of high temperature and low strain rate is more conducive to a better microstructure of 316LN. The best hot-working condition for 316LN in the range of experimental deformation parameters appears at $T = 1200$ °C and $\dot{\varepsilon} = 0.001$ s^{-1}.

Acknowledgments

The authors acknowledge China National Erzhong Group Co. for providing the experimental material and the financial support.

References

1. J.A. DeAlmeida and R. Barbosa, Hot Deformation of Austenitic Stainless Steel Type 316 up to Strain Rates of 100 s^{-1}, *ISIJ Int.*, 2005, **45**(2), p 296–298
2. M. Jafari and A. Najafizadeh, Correlation between Zener–Hollomon Parameter and Necklace DRX During Hot Deformation of 316 Stainless Steel, *Mater. Sci. Eng. A*, 2009, **501**(1–2), p 16–25
3. N.D. Ryan and H.J. McQueen, Hot Strength and Microstructural Evolution of 316 Stainless Steel During Simulated Multistage Deformation by Torsion, *J. Mater. Process. Technol.*, 1993, **36**(2), p 103–123
4. S.-I. Kim, Y.S. Lee, and B.-L. Jang, Modeling of Recrystallization and Austenite Grain Size for AISI, 316 Stainless Steel and Its Application to Hot Bar Rolling, *Mater. Sci. Eng. A*, 2003, **357**(1–2), p 235–239
5. H.J. McQueen and N.D. Ryan, Constitutive Analysis in Hot Working, *Mater. Sci. Eng. A*, 2002, **322**(1–2), p 43–63
6. J.Y. Xiang, R.B. Song, and P.D. Ren, 316L 不锈钢动态再结晶行为 (Dynamic Recrystallization Behavior of 316L Stainless Steel), *J. Univ. Sci. Technol. Beijing*, 2009, **31**(12), p 1555–1559 (in Chinese)
7. M.F. Abbod, C.M. Sellars, A. Tanaka, D.A. Linkens, and M. Mahouf, Effect of Changing Strain Rate on Flow Stress During Hot Deformation of Type 316L Stainless Steel, *Mater. Sci. Eng. A*, 2008, **491**(1–2), p 290–296
8. G.Q. He, C.S. Chen, and Q. Gao, 316L, 316LN 奥氏体不锈钢的单轴低周疲劳特性及其微结构 (The Characteristic and Microstructure of Uniaxial Low Cycle Fatigue of 316L and 316LN Austenitic Stainless Steels), *J. Southwest Jiaotong Univ.*, 1996, **31**(3), p 283–287 (in Chinese)
9. Y.L. Xu, J.Q. Zhang, F.M. Zhu, and A. Gessi, 国产 316LN 不锈钢在动态 Pb-Bi 中的腐蚀 (The Corrosion of Domestic 316LN Stainless Steel in Dynamic Pb-Bi). Annual of China Atomic Energy Science Research Institute, 2008, p 10–12 (in Chinese)
10. N.S. Bharasi, K. Thyagarajan, H. Shaikh, A.K. Balamurugan, Santanu. Bera, S. Kalavathy, K. Gurumurthy, A.K. Tyagi, R.K. Dayal, K.K. Rajan, and H.S. Khatak, Effect of Flowing Sodium on Corrosion and Tensile Properties of AISI, Type 316LN Stainless Steel at 823 K, *J. Nucl. Mater.*, 2008, **377**(2), p 378–384
11. T.S. Byun, E.H. Lee, and J.D. Hunn, Plastic Deformation in 316LN Stainless Steel—Characterization of Deformation Microstructures, *J. Nucl. Mater.*, 2003, **321**(1), p 29–39
12. D.W. Kim, J.H. Chang, and W.S. Ryu, Evaluation of the Creep-Fatigue Damage Mechanism of Type 316L and Type 316N Stainless Steel, *Int. J. Press. Vessel Pip.*, 2008, **85**(6), p 378–384
13. J.P. Strizak, H. Tian, P.K. Liaw, and L.K. Mansur, Fatigue Properties of Type 316LN Stainless Steel in Air and Mercury, *J. Nucl. Mater.*, 2005, **343**(1–3), p 134–144
14. J. Ganesh Kumar, M. Chowdary, V. Ganesan, R.K. Paretkar, K. Bhanu Sankara Rao, and M.D. Mathew, High Temperature Design Curves for High Nitrogen Grades of 316LN Stainless Steel, *Nucl. Eng. Des.*, 2010, **240**(6), p 1363–1370
15. J.Q. Xiong, G. Xie, and G.B. Tang, Research on Dynamic Recrystallization of Austenite and Flow Stress during Hot Deformation Process of 304 Stainless Steel (304 不锈钢热变形过程奥氏体动态再结晶及流变应力研究), *Yunnan Metall.*, 2008, **37**(5), p 37–42 (in Chinese)
16. W. Bingxin, W. Jiafu, L. Xianghua, and W. Guodong, Dynamic Recrystallization and Grain Refinement in a New Mn-Cr Gear Steel. 新型 Mn-Cr 齿轮钢的动态再结晶及晶粒细化, *J. Iron Steel Res.*, 2006, **18**(5), p 38–41 (in Chinese)
17. C.M. Sellars and W.J. McTegart, On the Mechanism of Hot Deformation, *Acta Metall*, 1966, **14**(9), p 1136–1138
18. C. Zener and J.H. Hollomon, Effect of Strain-Rate Upon the Plastic Flow of Steel, *J. Appl. Phys.*, 1944, **15**(1), p 22–32
19. Y.Q. Bai, M.M. Chen, and H.Q. Chen, 316LN 热变形行为及动态再结晶晶粒的演变规律 (Hot Deformation and Dynamic Recrystallization Behaviors of 316LN), *J. Taiyuan Univ. Sci. Technol.*, 2009, **30**(5), p 424–427 (in Chinese)
20. Y.V.R.K. Prasad, H.L. Gegel, S.M. Doraivelu, J.C. Malas, J.T. Morqan, K.A. Lark, and D.R. Barker, Modeling of Dynamic Materials Behavior in Hot Deformation: Forging of Ti-6242, *Metall. Mater. Trans. A*, 1984, **15**(10), p 1883–1892
21. Y.V.R.K. Prasad and S. Sasidharas, *Hot Working Guide: A Compendium of Processing Map*, 1st ed., Y.V.R.K. Prasad and S. Sasidharas, Ed., ASM International, Materials Park, OH, 1997, p 3–23
22. H.L. Gegel, J.C. Malas, and S.M. Doraivelu, Process Modelling of p/m Extrusion, *Innovations in Materials Processing*, G. Bruggeman and V. Weiss, Ed., Plenum Press, New York, 1985, p 137–140